Sci. Bull. (2016) 61(2):116–124
DOI 10.1007/s11434-015-0968-8

www.scibull.com
www.springer.com/scp

Review

Earth Sciences

Mass-independent fractionation of even mercury isotopes

Hongming Cai · Jiubin Chen

Received: 9 September 2015 / Revised: 12 November 2015 / Accepted: 27 November 2015 / Published online: 29 December 2015

Abstract Practically all physical, chemical, and biological processes can induce mass-dependent fractionation of mercury (Hg) isotopes. A few special processes such as photochemical reduction of Hg(II) and photochemical degradation of methylmercury (MeHg) can produce mass-independent fractionation (MIF) of odd Hg isotopes (odd-MIF), which had been largely reported in variable natural samples and laboratory experiments, and was thought to be caused by either nuclear volume effect or magnetic isotope effect. Recently, intriguing MIF of even Hg isotopes (even-MIF) had been determined in natural samples mainly related to the atmosphere. Though photo-oxidation in the tropopause (inter-layer between the stratosphere and the troposphere) and neutron capture in space were thought to be the possible processes causing even-MIF, the exact mechanism triggering significant even Hg isotope anomaly is still unclear. Even-MIF could provide useful information about the atmospheric chemistry and related climate changes, and the biogeochemical cycle of Hg.

Keywords Mass-independent fractionation · Even mercury isotopes · Processes producing even-MIF · Mechanisms triggering even-MIF · Self-shielding · Neutron capture

H. Cai · J. Chen (✉)
State Key Laboratory of Environmental Geochemistry, Institute of Geochemistry, Chinese Academy of Sciences, Guiyang 550081, China
e-mail: chenjiubin@vip.gyig.ac.cn

H. Cai
University of Chinese Academy of Sciences, Beijing 100049, China

1 Introduction

Mercury (Hg) is a globally distributed and highly toxic pollutant [1–3]. It virtually exists in all natural ecosystems on earth. In recent years, more and more Hg has been emitted into earth's biogeochemical system by human activities such as the burning of fossil fuel and cement production [4]. Unlike other heavy metals, Hg has a stable gaseous form (Hg^0) that has a residence time of ~1 year in the atmosphere [5, 6]. Thus, Hg released by point sources can be transported far from the sources in the atmosphere and may affect the ecosystems even in remote regions after deposition (e.g., the Arctic and Antarctic) [7–12]. More importantly, mercury can be methylated into neurotoxic and bioaccumulative methylmercury (MeHg), which can pose serious threat to the human health via fish or rice consumption [13–15]. Therefore, it is critical to fully understand the source, transformation, and fate of Hg in the environment in order to appropriately target the remediation of Hg contamination and maintain emission of Hg at the sustainable levels [16]. Although significant progress has been made in previous research on Hg biogeochemical cycle, many processes involved in Hg transformation and dispersion in variable ecosystems still remain unidentified or unquantified. Some new approaches are thus needed to be developed for better understanding the conundrums of identifying Hg source and ascertaining Hg fate in the environment. The recently developed Hg stable isotope method sheds new insight into tracing pollution sources and behavior of Hg in nature [7, 17–21].

To date, more than 100 papers have been published on Hg isotope ratios, which demonstrated the potential of Hg isotope in tracing the source, processes and the fate of Hg in the atmosphere, biosphere, lithosphere, and hydrosphere [22].

These studies have reported very large mass-dependent fractionation (MDF, δ^{202}Hg) of Hg isotopes in natural samples (up to 20 ‰ of δ^{202}Hg) due to its active chemical property. In addition to MDF, recent studies reported significant mass-independent fractionation (MIF, Δ^{199}Hg and Δ^{201}Hg) of odd Hg isotopes (odd-MIF) in natural samples, rendering Hg, a heavy metal having significant MIF in nature [3, 7, 23–25]. The magnetic isotope effect (MIE) and the nuclear volume effect (NVE) are thought to be the most possible mechanisms causing such odd-MIF [3, 26–35]. Unlike MDF, only a few processes can cause odd-MIF, such as photochemical reduction, abiotic dark reduction, evaporation, and photodegradation [3, 30, 31, 34].

Intriguingly, MIF of even isotopes (even-MIF) has recently been observed mainly in atmospheric samples (up to +1.24 ‰) [24, 36–42]. Since no even-MIF was reported in laboratory experiments up to now and the two causes of odd-MIF (MIE and NVE) unlikely produce significant even-MIF [27, 32, 36, 38, 43], the mechanisms and the processes triggering even-MIF remain unclear. Interestingly, only samples related to the atmosphere display such even isotope anomaly, indicating the potential of even-MIF as a useful tracer of upper atmosphere contribution.

Several papers have previously reviewed Hg isotope systematics [7, 20–22, 44–46]. Here, we give a careful review of publications on even Hg isotope anomalies, with a main focus on sample strategies and possible processes and mechanisms triggering MIF of even Hg isotopes. Our newly measured results from Tibetan and Guiyang precipitation were also added in the data set to show that even-MIF is a phenomenon largely distributed in the world.

2 Mercury isotope ratio nomenclature

Hg has seven stable isotopes: ^{196}Hg, ^{198}Hg, ^{199}Hg, ^{200}Hg, ^{201}Hg, ^{202}Hg, and ^{204}Hg, with approximate abundance of 0.155 %, 10.04 %, 16.94 %, 23.14 %, 13.17 %, 29.73 %, and 6.83 %, respectively. Mass-dependent fractionation (MDF) refers to the fact that the distribution of different Hg isotopes in variable materials or phases is proportional to their isotopic masses during the physical, chemical, and biological processes. The MDF of Hg isotopes is expressed as δ (‰) notation defined as:

$$\delta^{x}\mathrm{Hg} = [(^{x}\mathrm{Hg}/^{198}\mathrm{Hg})_{\mathrm{sample}}/(^{x}\mathrm{Hg}/^{198}\mathrm{Hg})_{\mathrm{std}} - 1] \times 1000, \quad (1)$$

where x represents 199, 200, 201, 202, and 204 amu, std is the international NIST SRM 3133 standard suggested by Blum and Bergquist [47].

The MIF refers to any chemical or physical process that aims to separate isotopes, where the amount of separation is not in proportion to different mass of the isotopes [48]. MIF is reported in "capital delta" notation (Δ^{x}Hg; the deviation from MDF in units of per mil, ‰), calculated from the differences between the measured isotope value and the theoretically predicted isotope value using the MDF fractionation law:

$$\Delta^{199}\mathrm{Hg} = \delta^{199}\mathrm{Hg} - 0.252 \times \delta^{202}\mathrm{Hg}, \quad (2)$$

$$\Delta^{200}\mathrm{Hg} = \delta^{200}\mathrm{Hg} - 0.502 \times \delta^{202}\mathrm{Hg}, \quad (3)$$

$$\Delta^{201}\mathrm{Hg} = \delta^{201}\mathrm{Hg} - 0.752 \times \delta^{202}\mathrm{Hg}, \quad (4)$$

$$\Delta^{204}\mathrm{Hg} = \delta^{204}\mathrm{Hg} - 1.493 \times \delta^{202}\mathrm{Hg}. \quad (5)$$

Blum and Bergquist [47] had measured the isotopic composition of UM-Almaden and suggested that all laboratories adopt UM-Almaden as a secondary standard to get consensus values and correct the analytical bias.

3 Mainstream observation of odd-MIF

The odd-MIF were reported in a large set of environmental, geological, and biological samples, including atmospheric samples [23–25, 36–39, 42, 49, 50], sediments [49, 51–67], soils [37, 68–70], peats [71], rocks [72], coals [24, 68, 73, 74], mosses and lichens [50, 75–77], human hairs [78–80], plants [37, 50, 81], fishes [3, 62, 78, 80–83], and even seabirds [53, 84]. Blum et al. [22] have given a detail description of these data in a recent review article.

The odd-MIF has been proven to occur in laboratory experiments. Bergquist and Blum [3] firstly studied Hg isotopic fractionation during the photoreduction of Hg(II) and photodegradation of MeHg. Their results showed that the residual Hg(II) was enriched in odd Hg isotopes. Zheng and Hintelmann [33] found that the photoreduction of Hg(II) was controlled by Hg/DOC ratio, and the reactant Hg(II) was enriched in ^{199}Hg and ^{201}Hg. Different types of ligands may induce opposite magnetic isotope effects during photochemical processes. For example, Zheng and Hintelmann [35] showed that during the photochemical processes of S-containing ligands, magnetic isotopes (^{199}Hg and ^{201}Hg) were specifically enriched in the product (Hg^0) rather than in the reactant Hg(II). Odd-MIF was also reported in abiotic processes. During the evaporation of liquid Hg, a small positive Δ^{199}Hg was observed in gaseous elemental Hg (Hg^0) [31, 32]. Zheng and Hintelmann [34] also reported a small positive odd-MIF in the reactant during the abiotic dark reduction of Hg(II).

Unlike MDF of Hg isotopes that occur in most of equilibrium and kinetic processes, odd-MIF has only been found in several specific processes (see above discussion). The nuclear volume effect and the magnetic isotope effect were thought to be the two possible mechanisms triggering odd-

MIF [3, 26–28, 30–32, 34]. The MIE is caused by angular momentum of electrons and magnetic nuclei. Among all seven isotopes of Hg, only odd isotopes ^{199}Hg and ^{201}Hg have nuclear spins and magnetic moments. As a result, MIE can only affect ^{199}Hg and ^{201}Hg isotopes [22, 29]. The NVE was proposed by Bigelesen et al. (1996) to explain the unusual fractionation of odd U isotopes observed by Fujii et al. (1989) that cannot be explained by the classical MDF theory of chemical isotope effect [26, 85]. The NVE is related to the difference in nuclear shapes and sizes of isotopes. In general, nuclear radius and mass are both proportional to the number of neutrons in an isotope. However, the odd isotopes ^{199}Hg and ^{201}Hg have slightly smaller nuclear charge radii than expected, which leads to the ground-state energies of odd isotopes closer to the adjacent lower even isotopes [3, 32, 86]. As a result, isotopic fractionation may be triggered by the even–odd difference that will not correlate with the difference in mass [26]. The NVE is negligible for light elements, but can be significant for heavy elements such as Hg, Pb, Tl, and U [32].

4 Observation of even-MIF in natural samples

The observation of even-MIF is intriguing and provides new insight into Hg stable isotope systematics. Recently, several studies have reported significant MIF of even-mass-number isotopes of Hg (^{200}Hg and ^{204}Hg) mainly in atmospheric samples [24, 36–42]. Gratz et al. [38] first reported a positive MIF of ^{200}Hg (Δ^{200}Hg less than +0.25 ‰) in precipitation samples [mainly Hg(II)] coupled with slightly negative MIF of ^{200}Hg in vapor-phase samples in the Great Lakes region, USA (mean Δ^{200}Hg = −0.04 ‰ ± 0.09 ‰, 2SD). Subsequently, Chen et al. [36] confirmed the presence of larger magnitude of Δ^{200}Hg (up to +1.24 ‰) in snow and rain samples in Peterborough (ON, Canada) and found a definite seasonal variation of Δ^{200}Hg, with relatively higher values in winter but lower in summer. Demers et al. [37] observed positive Δ^{200}Hg (mean Δ^{200}Hg = 0.18 ± 0.05 ‰, 1SD) in precipitation but negative Δ^{200}Hg (mean Δ^{200}Hg = −0.1 ‰ ± 0.02 ‰, 1SD) in total gaseous mercury in Wisconsin, USA. On the contrary, the same samples displayed negative Δ^{204}Hg in precipitation (mean Δ^{204}Hg = −0.25 ‰ ± 0.21 ‰, 1SD) but positive Δ^{204}Hg in total gaseous mercury (mean Δ^{204}Hg = 0.13 ‰ ± 0.05 ‰, 1SD). Rolison et al. [39] reported similar results in atmospheric samples of a coastal environment in Florida, USA, with negative Δ^{200}Hg (from −0.19 ‰ to −0.06 ‰) in gaseous elemental Hg (Hg^0) but positive Δ^{200}Hg (from +0.06 ‰ to +0.28 ‰) in reactive gaseous Hg ($Hg^{II}_{(g)}$) and particle-bound Hg (Hg_p). Mead et al. [43] documented unusual values for ^{200}Hg anomalies (up to −10.69 ‰) and Δ^{204}Hg (up to 27.57 ‰) in the special compact fluorescent lamp (also all odd isotopes), where the intensity of illumination and Hg concentration are much higher than natural environment. Štrok et al. [40] found a positive Δ^{200}Hg value (up to 0.50 ‰) in seawater from the Canadian Arctic Archipelago. Recently, Wang et al. [41] also reported a relatively smaller positive Δ^{200}Hg values (up to 0.20 ‰) in precipitation collected in Guiyang, China.

5 Hidden alternate systematics of even-MIF

The even-MIF may also occur for other even isotopes. As mentioned above, even-MIF is expressed as Δ^xHg, where x can represent 196, 198, 200, 202, and 204. Since ^{202}Hg/^{198}Hg ratio is arbitrarily chosen for describing MDF, and the MIF of Hg isotopes were calculated based on 202/198 ratio, so other even Hg isotopes may also fractionate in a mass-independent manner including ^{202}Hg and ^{198}Hg themselves. However, due to the design limitation of the first generation MC-ICP-MS and the very low abundance of ^{196}Hg (thus the low sensitivity), only Δ^{200}Hg and Δ^{204}Hg were calculated and reported in some previous studies.

In the following, even Hg isotope anomalies will be recalculated in order to explore the alternative even-MIF systematics. We can choose ^{202}Hg as the denominator in δ^xHg expression and calculate the $\Delta^{200/202}$Hg value. Similarly, we can obtain $\Delta^{198/200}$Hg value using ^{200}Hg as a denominator:

$$\delta^x\mathrm{Hg} = [(^x\mathrm{Hg}/^{200}\mathrm{Hg})_{\mathrm{sample}}/(^x\mathrm{Hg}/^{200}\mathrm{Hg})_{\mathrm{std}} - 1] \times 1000, \quad (6)$$

$$\delta^x\mathrm{Hg} = [(^x\mathrm{Hg}/^{202}\mathrm{Hg})_{\mathrm{sample}}/(^x\mathrm{Hg}/^{202}\mathrm{Hg})_{\mathrm{std}} - 1] \times 1000, \quad (7)$$

where x represents 198, 199, 200, or 201. $\Delta^{198/200}$Hg and $\Delta^{200/202}$Hg can thus be calculated using the following Eqs. (8) and (9), respectively [87]:

$$\Delta^{198/200}\mathrm{Hg} = \delta^{198/200}\mathrm{Hg} - (-1.0097) \times \delta^{202/200}\mathrm{Hg}, \quad (8)$$

$$\Delta^{200/202}\mathrm{Hg} = \delta^{200/202}\mathrm{Hg} - 0.4976 \times \delta^{198/202}\mathrm{Hg}. \quad (9)$$

The recalculated $\Delta^{198/200}$Hg and $\Delta^{200/202}$Hg using Eqs. (8) and (9) for the same data reported in Chen et al. [36] are shown in Fig. 1. The recalculated result displayed even higher values for MIF of ^{198}Hg or ^{200}Hg isotopes (Fig. 1). Interestingly, all rain or snow samples displayed negative $\Delta^{198/200}$Hg (from −0.41 to −2.47 ‰) but positive values of $\Delta^{200/202}$Hg (from +0.21 to +1.24 ‰) and an obvious seasonal variation in $\Delta^{198/200}$Hg or $\Delta^{200/202}$Hg.

Alternatively, we can also calculate the even isotope anomalies using an odd isotope (e.g., ^{199}Hg) as numerator and an even isotope (e.g., ^{198}Hg) as a denominator in the

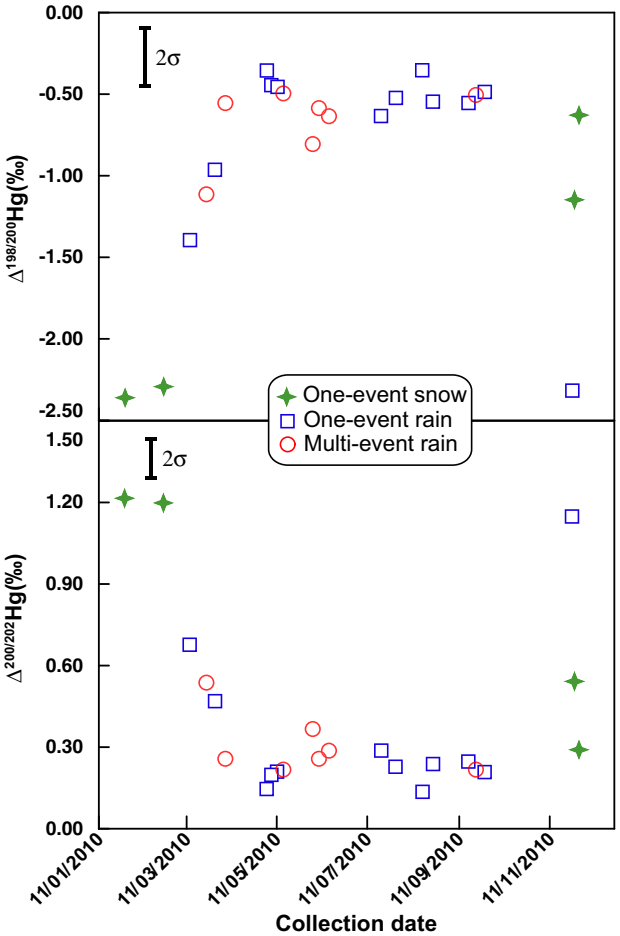

Fig. 1 Recalculated $\Delta^{198/200}$Hg and $\Delta^{200/202}$Hg values using even/even isotope ratio for the same precipitation samples collected in Peterborough, Ontario, Canada [36]

δ^{x}Hg definition, and the even-MIF can thus be defined for ^{200}Hg, ^{202}Hg and ^{204}Hg by the following equations [87]:

$$\Delta^{200/198}\mathrm{Hg} = \delta^{200/198}\mathrm{Hg} - 1.9935 \times \delta^{199/198}\mathrm{Hg}, \quad (10)$$

$$\Delta^{202/198}\mathrm{Hg} = \delta^{202/198}\mathrm{Hg} - 3.9679 \times \delta^{199/198}\mathrm{Hg}, \quad (11)$$

$$\Delta^{204/198}\mathrm{Hg} = \delta^{204/198}\mathrm{Hg} - 5.9234 \times \delta^{199/198}\mathrm{Hg}. \quad (12)$$

Figure 2 shows a linear relationship between $\Delta^{200/198}$Hg and $\Delta^{202/198}$Hg calculated using odd/even isotope ratio for the same precipitation samples reported in Chen et al. [36].

Therefore, given the conventional calculation of Δ^{200}Hg ($\Delta^{200}\mathrm{Hg} = \delta^{200}\mathrm{Hg} - \delta^{202}\mathrm{Hg} \times 0.502$), it cannot allow us to identify which of the three even isotopes (^{198}Hg, ^{200}Hg and ^{202}Hg) is anomalous. In fact, it is suspected that all even isotopes are controlled by the same fractionating process and thus are subject to fractionation that does not change linearly with mass (Fig. 2). Moreover, the simultaneous measurements of ^{204}Hg and ^{196}Hg are also necessary and helpful in answering such question. However, in

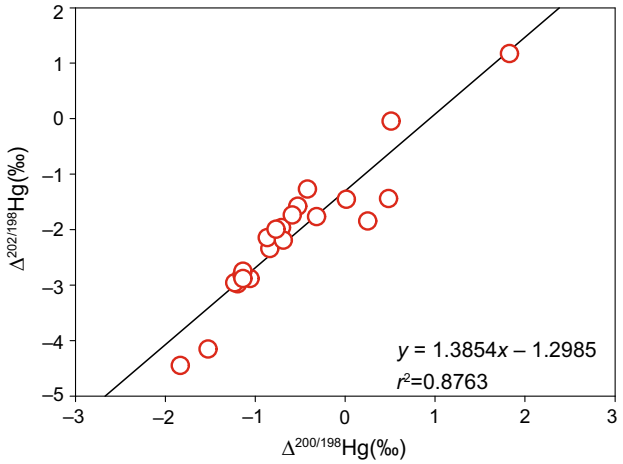

Fig. 2 Relationship between $\Delta^{200/198}$Hg and $\Delta^{202/198}$Hg for the same precipitation samples collected in Peterborough, Ontario, Canada [36]. The data were recalculated using odd/even isotope ratio

the absence of a clearer understanding of the underlying mechanism, we can only pretend at this stage that the calculative deviations reported in recent studies are due to the anomalous behavior of ^{200}Hg, but it should be understood that any or all of the even isotopes may be contributed to the observed results. Obviously, the Hg isotope system is extremely complex and we have a long way for fully understanding its intricacies [36].

6 Pre-treatment methods used for discovering even-MIF

Three pre-treatment methods have been used in previous studies in which even-MIF has been found. The first method was a chromatographic pre-concentration method [88], which was used in the study of Hg isotopes in precipitation from Peterborough, ON, Canada [36], and in rain samples in Guiyang and Tibetan Plateau, China [41, 42]. Using this method, pre-treated (acidified and BrCl-digested) water samples were loaded onto a chromatographic column charged with 0.5-ml AG 1-X4 resin. After the removal of matrix, Hg was finally eluted with 10 mL 0.5 mol/L HNO_3 containing 0.05 % L-cysteine for final isotopic measurement on MC-ICP-MS [88]. In addition, solutions, which were prepared with NIST SRM 3133 Hg and TraceCERT ICP standard Hg, were also processed using the same protocol to confirm that laboratory manipulation and isotopic measurement themselves do not induce any ^{200}Hg anomaly [36]. Štrok et al. [89] developed an analogous method for the pre-concentration of Hg from large volumes of seawater. After digesting, seawater was loaded onto pre-cleaned anion exchange column for pre-concentrating Hg, and Hg that adsorbed on the resin was

finally eluted by 0.05 % L-cysteine in sodium citrate dehydrate [89]. The second method was employed by Gratz et al. [38] for the pre-treatment of precipitation samples in the Great Lakes region. During the procedure, the BrCl-digested sample was first reduced by agents containing 10 % $SnCl_2$, 50 % H_2SO_4, and 1 % NH_2OH in a frosted-tip gas–liquid separator. The reduced $Hg^0_{(g)}$ was then trapped in 25 g of 2 % $KMnO_4$ solution for isotopic measurement. The third method was mainly composed of a thermal combustion stage followed by a solution trapping and was used in several studies on Hg isotopes in the atmosphere [37–39]. In this method, gaseous elemental Hg ($Hg^0_{(g)}$), reactive gaseous Hg($Hg^{II}_{(g)}$) and aerosol Hg($Hg_{(p)}$) that were either trapped onto gold traps or collected on filters were first thermally released (by slowly heating to >500 °C) and then transferred by argon or nitrogen gases into a trap solution (e.g., $KMnO_4$-contained solution). The final solution was ready for Hg isotopic measurement [37–39].

We mentioned here that, in most of these studies, the methods were of course carefully calibrated and validated in order to accurately determine Hg isotopes in natural samples. Though a few studies reported incomplete recovery of Hg in some samples, it would not induce any even isotope anomaly [36]. Moreover, the isotopic measurement on MC-ICP-MS instrument itself could also not produce any MIF. Thus, the discoverable MIF of even Hg isotopes was unlikely a phenomenon induced by artificial manipulation. As a result, even-MIF does exist in nature.

7 Processes inducing MIF of even Hg isotopes

Though significant odd-MIF was induced by processes such as photo-reduction, photo-degradation, abiotic dark reduction, and evaporation, no ^{200}Hg anomalies have been reported during these interactions [3, 30, 31, 33, 34, 90]. This suggests that even-MIF is likely triggered by different bio-geological processes. This can probably be confirmed by the fact that Δ^{199}Hg and Δ^{200}Hg displayed contrasting seasonal variations in Chen et al. [36]. Since almost all samples that displayed ^{200}Hg anomalies are related to atmospheric Hg, even-MIF may be somehow produced in the atmosphere [24, 36–39, 41, 42].

Chen et al. [36] proposed a conceptual model for explaining even-MIF occurrence based on the geochemical parameters of precipitation samples and the air mass trajectories. As ^{200}Hg anomaly exists mainly in Hg(II) phase of precipitation samples and the main gaseous Hg phase is characterized by close to zero or slightly negative Δ^{200}Hg, and subsequent mainly physical processes (scavenging into droplets or onto particle) are unlikely to produce MIF, the even-MIF seems to derive from specific oxidation of Hg^0 to Hg(II) (RGM or Hg_p). The back trajectory model showed that the air masses of samples with relatively higher Δ^{200}Hg (e.g., winter snow) mainly came from the interlayer between stratosphere and troposphere (tropopause), which is characterized by high content of oxidants such as H_2O_2, ozone, hydroxyl, and halogen radicals and intense UV irradiation, both favoring the oxidation of Hg^0 [5, 36, 91–94]. It is therefore likely that even-MIF occurs in the tropopause. In fact, the large presence of snow crystals and frozen aerosols in the tropopause may serve as the potential vectors that capture both oxidants and Hg^0 to facilitate Hg^0 oxidation. After interaction, the Hg with ^{200}Hg anomaly could be transported downward by stratosphere-to-troposphere incursion to the surface (Fig. 3). Since the troposphere was shallower in the high latitude region (e.g., the North Pole) than the low latitude region, the intensity of stratosphere-to-troposphere invasion will decrease toward lower latitude region. In fact, even-MIF of all precipitation samples worldwide, including our unpublished Δ^{200}Hg data from the Tibetan Plateau (China), displayed a general increase with latitude, confirming the upper atmosphere as the possible origin of even-MIF (Fig. 4) [24, 36–39, 41, 42].

Additionally, even-MIF was also found for Hg trapped in the glass wall of compact fluorescent lamp (CFL) [43]. During lamp use, a small fraction of Hg, which comes from Hg amalgam pellet in the CFL, was trapped within the glass wall. Mead et al. [43] found significant unusual fractionation of even Hg isotopes between the trapped Hg pool (Hg contained within the glass wall) and the bulk Hg reservoir (comprising Hg amalgam pellet, Hg vapor, and adsorbed Hg), with $\Delta^{200}\text{Hg} = -10.69$ ‰ in the wall-trapped inventory. At the same time, unusual odd Hg isotope anomaly were also observed in used lamps, with $\Delta^{199}\text{Hg} = -21.49$ ‰ and $\Delta^{201}\text{Hg} = 13.42$ ‰. These lamps had been approved to be a closed system by mass balance of Hg. Because the amount of trapped Hg was less than 1 % of the bulk Hg in the lamps, the fractionation in trapped Hg should be roughly 100 times larger than of the bulk Hg. Obviously, NVE or MIE cannot explain this opposite trend between Δ^{199}Hg and Δ^{201}Hg. Another process or mechanism might contribute to the unusual Hg isotopes fractionation in CFL.

8 Possible mechanisms triggering MIF of even Hg isotopes

As we discussed above, of all seven isotopes of Hg, only odd isotopes ^{199}Hg and ^{201}Hg have nonzero nuclear spins and magnetic moments, and the NVE only can trigger negligible MIF of the even Hg isotopes [3, 32]. Therefore, MIE and NVE both could not induce significant MIF of even isotopes. Among the well-constrained mechanisms up

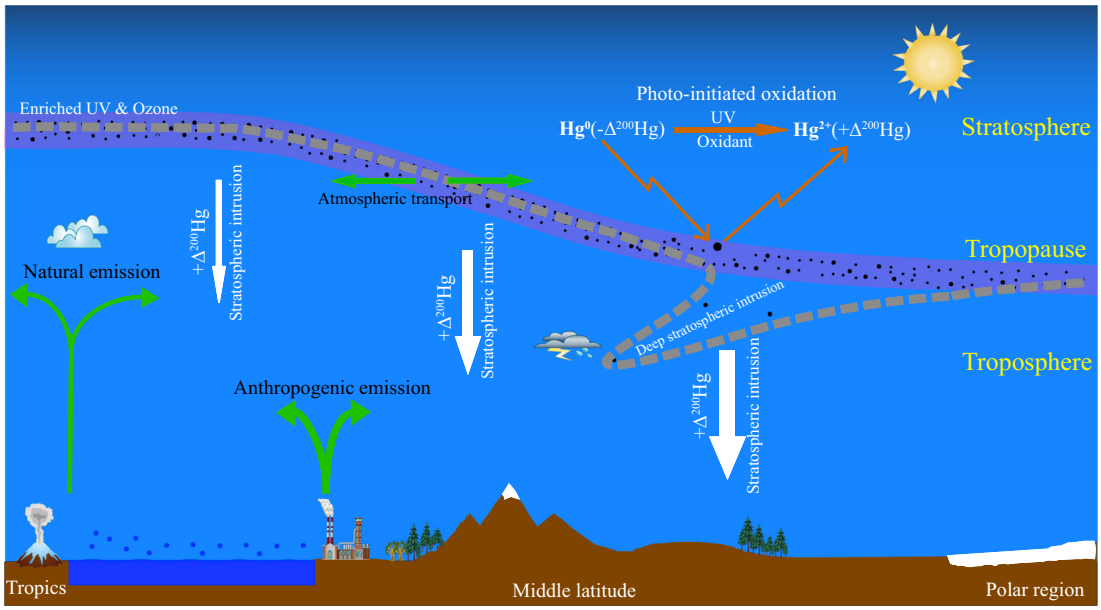

Fig. 3 Conceptual model of even-MIF formation and its transport to the surface ecosystems

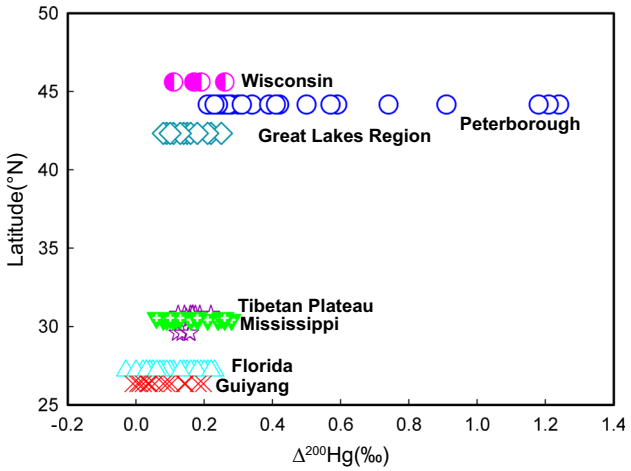

Fig. 4 Even-MIF in precipitation samples collected from the North America and China (modified from Wang et al. 2015) [24, 36–39, 41, 42]. The Wisconsin rain samples collected in summer are similar to those samples in Peterborough of the same season. The fact that Δ^{200}Hg displays a general increase with latitude implies an upper atmosphere provenance of even-MIF

to now, the self-shielding effect, known from O isotope systematics, and neutron capture may be possible causes of even-MIF.

8.1 Self-shielding

Mead et al. [43] suggested that the observed fractionation including even-MIF and odd-MIF in CFL likely results from the self-shielding effect. According to Mead et al. [43] and Sommerer [95], the hyperfine structure of the Hg absorption spectrum can lead to a self-shielding effect. Due to different nuclear spin and mass of the seven Hg isotopes, the Hg absorption line at 254 nm will split into 10 components, which can be reduced to six distinct lines through thermal and collisional broadening under CFL conditions. The specific transmittance at each line is related to the isotopic abundance and thus the transmittances at all lines are not identical. During Hg interaction, the six components mentioned above will be attenuated proportionally to their isotope abundances. Therefore, the abundant isotopes can "shield" themselves partially from photoexcitation because of attenuation. As a result, Hg isotopes with low abundance (e.g., ^{196}Hg) could be more easily photoexcited than those with high abundance (e.g., ^{202}Hg), inducing an unusual isotopic fractionation that does not change linearly with mass [43, 95]. In this case, ^{196}Hg has the highest emission/absorption ratio, while ^{202}Hg has the lowest due to their lowest and highest abundances, respectively. Mead et al. [43] showed that the combined fractionation factors induced by both self-shielding and MDF could roughly describe the features of the measured data; either NVE or MIE would not significantly improve the match of calculated result with observation. Therefore, self-shielding is the most possible mechanism creating even-MIF. However, given the fact that Hg concentration is very low in the atmosphere and the sunshine has a different spectrum from CFL, direct evidence is needed to confirm the self-shielding as an appropriate cause of even-MIF in nature. In fact, the anomalies resulted from self-shielding will be proportional to the isotope abundances, which is inconsistent with the actual observation [37–41].

8.2 Neutron capture

In addition to self-shielding, neutron capture may be another mechanism potentially explaining the observed ^{200}Hg anomalies. The neutron capture cross section is used to express the likelihood of interaction between an incident neutron and a target nucleus. The values of capture cross section are 3,080 ± 180, 2.0 ± 0.3, 2,150 ± 48, <60, 5.7 ± 1.2, and 4.42 ± 0.07 barns for ^{196}Hg, ^{198}Hg, ^{199}Hg, ^{200}Hg, ^{201}Hg, and ^{202}Hg, respectively [96]. Obviously, the capture cross section of ^{199}Hg is much higher (>99.9 % of the total Hg neutron cross section) than those of other Hg isotopes except for ^{196}Hg which has the lowest abundance and therefore not measurable at this stage [96–98]. In other words, it is much easier for ^{199}Hg to capture neutron and then transform into larger mass number Hg isotopes, with a large possibility to ^{200}Hg. Thus, the neutron capture reactions occurred in a reservoir with natural Hg isotopes would result in positive Δ^{200}Hg but corresponding negative ^{199}Hg anomalies. This could explain at least part of the inverse correlation feature of the data reported by Chen et al. [36]. However, the neutron capture generally takes a very long time (about millions of years) to significantly change the isotope distribution, and this would unlikely happen in the higher atmosphere due to a very short lifetime of Hg in atmosphere (about ~1 year). One possibility is the presence of an extremely old Hg pool somewhere in the space that is frequently affected by neutron capture reactions. The fact that Hg released from this possible old Hg pool (thus with ^{200}Hg anomaly) from time to time would leak into the lower layers (e.g., by stratosphere–troposphere transport events) could eventually cause positive ^{200}Hg anomalies in precipitation samples. However, it is still not clear whether the presence of such an old Hg pool in the upper atmosphere is true or not. Anyway, without direct evidence, the cause of neutron capture for even-MIF remains as a speculation.

9 Conclusion and implication

This paper reviews the recent publication on the MIF of even-mass Hg isotopes. The definition and possible processes and mechanisms triggering even-MIF were carefully discussed. Given the fact that even isotope anomaly was observed in variable regions with different altitude and latitude in China and in North America, the occurrence of even-MIF is likely a worldwide phenomenon. This is also supported by the positive Δ^{200}Hg (~+0.22 ‰) just determined in the tree moss in Sweden (our unpublished data). Though Δ^{200}Hg is actually used to refer to the deviation of even Hg isotopes from MDF, other even isotopes are probably subject to the same fractionation. The relationships among even isotope anomalies need to be fully elucidated. In general, Δ^{200}Hg values were mainly determined in samples related to the atmosphere, implying an upper atmosphere origin of even-MIF. Laboratory experiments, theoretical contribution and more data are needed to fully understand the reactions and mechanisms triggering even-MIF. If the conceptual model of Chen et al. [36] can hold, even-MIF may serve as a useful indicator of upper atmosphere chemistry. The implication of even-MIF as a possible conservative tracer remains to be largely developed. In fact, ^{200}Hg anomaly is likely related to solar irradiation, air mass move, and stratosphere incursion, and thus even-MIF could provide additional information about atmospheric chemistry, meteorological condition, and even related climate changes. Moreover, the conservative behavior of ^{200}Hg anomaly may also be helpful for better understanding the global biogeochemical cycle of Hg, especially the surface–atmosphere exchange.

Acknowledgments This work was supported by the Natural Science Foundation of China (41273023, U1301231), the National Basic Research Program of China (2013CB430001), the Strategic Priority Research Program (XDB05030302), the "Hundred Talent" Project of Chinese Academy of Sciences and SKLEG. We thank Y. Liu, H.-M. Bao, H. Hintelmann, Meili M, and J. Wiederhold for constructive discussion.

References

1. Fitzgerald WF, Engstrom DR, Mason RP et al (1998) The case for atmospheric mercury contamination in remote areas. Environ Sci Technol 32:1–7
2. Lamborg CH, Fitzgerald WF, Damman AWH et al (2002) Modern and historic atmospheric mercury fluxes in both hemispheres: global and regional mercury cycling implications. Glob Biogeochem Cycles 16:51-1–51-11
3. Bergquist BA, Blum JD (2007) Mass-dependent and -independent fractionation of Hg isotopes by photoreduction in aquatic systems. Science 318:417–420
4. Mason RP, Sheu GR (2002) Role of the ocean in the global mercury cycle. Glob Biogeochem Cycles 16:40-1–40-14
5. Lin C-J, Pehkonen SO (1999) The chemistry of atmospheric mercury: a review. Atmos Environ 33:2067–2079
6. Lindqvist O, Rodhe H (1985) Atmospheric mercury—a review. Tellus B 37:136–159
7. Bergquist BA, Blum JD (2009) The odds and evens of mercury isotopes: applications of mass-dependent and mass-independent isotope fractionation. Elements 5:353–357
8. Landers D, Ford J, Gubala C et al (1995) Mercury in vegetation and lake sediments from the US Arctic. Water Air Soil Pollut 80:591–601
9. Lindberg SE, Brooks S, Lin CJ et al (2002) Dynamic oxidation of gaseous mercury in the Arctic troposphere at polar sunrise. Environ Sci Technol 36:1245–1256
10. Schroeder WH, Anlauf KG, Barrie LA et al (1998) Arctic springtime depletion of mercury. Nature 394:331–332
11. Schroeder WH, Markes J (1994) Measurements of atmospheric mercury concentrations in the Canadian environment near Lake Ontario. J Great Lakes Res 20:240–259
12. Schroeder WH, Munthe J (1998) Atmospheric mercury—an overview. Atmos Environ 32:809–822

13. Clarkson TW (1993) Mercury: major issues in environmental health. Environ Health Perspect 100:31–38
14. Feng X, Qiu G (2008) Mercury pollution in Guizhou, Southwestern China—an overview. Sci Total Environ 400:227–237
15. St. Louis VL, Hintelmann H, Graydon JA et al (2007) Methylated mercury species in Canadian high Arctic marine surface waters and snowpacks. Environ Sci Technol 41:6433–6441
16. Weiss DJ, Rehkdmper M, Schoenberg R et al (2008) Application of nontraditional stable-isotope systems to the study of sources and fate of metals in the environment. Environ Sci Technol 42:655–664
17. Blum JD (2011) Marine chemistry: marine mercury breakdown. Nat Geosci 4:139–140
18. Hintelmann H, Zheng W (2012) Environmental Chemistry and Toxicology of Mercury. In: Tracking geochemical transformations and transport of mercury through isotope fractionation, 1st edn. Wiley, New York, pp 293–327
19. Sonke JE (2011) A global model of mass independent mercury stable isotope fractionation. Geochim Cosmochim Acta 75:4577–4590
20. Yin R, Feng X, Li X et al (2014) Trends and advances in mercury stable isotopes as a geochemical tracer. Trends Environ Anal Chem 2:1–10
21. Yin R, Feng X, Shi W (2010) Application of the stable-isotope system to the study of sources and fate of Hg in the environment: a review. Appl Geochem 25:1467–1477
22. Blum JD, Sherman LS, Johnson MW (2014) Mercury isotopes in earth and environmental sciences. Annu Rev Earth Planet Sci 42:249–269
23. Sherman LS, Blum JD, Johnson KP et al (2010) Mass-independent fractionation of mercury isotopes in Arctic snow driven by sunlight. Nat Geosci 3:173–177
24. Sherman LS, Blum JD, Keeler GJ et al (2011) Investigation of local mercury deposition from a coal-fired power plant using mercury isotopes. Environ Sci Technol 46:382–390
25. Sherman LS, Blum JD, Douglas TA et al (2012) Frost flowers growing in the Arctic ocean-atmosphere–sea ice–snow interface: 2. Mercury exchange between the atmosphere, snow, and frost flowers. J Geophys Res Atmos 117:188–194
26. Bigeleisen J (1996) Nuclear size and shape effects in chemical reactions. Isotope chemistry of the heavy elements. J Am Chem Soc 118:3676–3680
27. Buchachenko A, Ivanov V, Roznyatovskii V et al (2007) Magnetic isotope effect for mercury nuclei in photolysis of bis (p-trifluoromethylbenzyl) mercury. Dokl Phys Chem 413:39–41
28. Buchachenko AL (2001) Magnetic isotope effect: nuclear spin control of chemical reactions. J Phys Chem A 105:9995–10011
29. Buchachenko AL (2009) Mercury isotope effects in the environmental chemistry and biochemistry of mercury-containing compounds. Russ Chem Rev 78:319
30. Estrade N, Carignan J, Sonke JE et al (2009) Mercury isotope fractionation during liquid–vapor evaporation experiments. Geochim Cosmochim Acta 73:2693–2711
31. Ghosh S, Schauble EA, Couloume GL et al (2013) Estimation of nuclear volume dependent fractionation of mercury isotopes in equilibrium liquid–vapor evaporation experiments. Chem Geol 336:5–12
32. Schauble EA (2007) Role of nuclear volume in driving equilibrium stable isotope fractionation of mercury, thallium, and other very heavy elements. Geochim Cosmochim Acta 71:2170–2189
33. Zheng W, Hintelmann H (2009) Mercury isotope fractionation during photoreduction in natural water is controlled by its Hg/DOC ratio. Geochim Cosmochim Acta 73:6704–6715
34. Zheng W, Hintelmann H (2010) Nuclear field shift effect in isotope fractionation of mercury during abiotic reduction in the absence of light. J Phys Chem A 114:4238–4245
35. Zheng W, Hintelmann H (2010) Isotope fractionation of mercury during its photochemical reduction by low-molecular-weight organic compounds. J Phys Chem A 114:4246–4253
36. Chen J, Hintelmann H, Feng X et al (2012) Unusual fractionation of both odd and even mercury isotopes in precipitation from Peterborough, ON, Canada. Geochim Cosmochim Acta 90:33–46
37. Demers JD, Blum JD, Zak DR (2013) Mercury isotopes in a forested ecosystem: implications for air-surface exchange dynamics and the global mercury cycle. Glob Biogeochem Cycles 27:222–238
38. Gratz LE, Keeler GJ, Blum JD et al (2010) Isotopic composition and fractionation of mercury in Great Lakes precipitation and ambient air. Environ Sci Technol 44:7761–7770
39. Rolison J, Landing W, Luke W et al (2013) Isotopic composition of species-specific atmospheric Hg in a coastal environment. Chem Geol 336:37–49
40. Štrok M, Baya PA, Hintelmann H (2015) The mercury isotope composition of Arctic coastal seawater. C R Geosci 347:368–376
41. Wang Z, Chen J, Feng X et al (2015) Mass-dependent and mass-independent fractionation of mercury isotopes in precipitation from Guiyang, SW China. C R Geosci 347:358–367
42. Yuan S, Zhang Y, Chen J et al (2015) Large variation of mercury isotope composition during a single precipitation event at Lhasa City, Tibetan Plateau, China. Procedia Earth Planet Sci 13:282–286
43. Mead C, Lyons JR, Johnson TM et al (2013) Unique Hg stable isotope signatures of compact fluorescent lamp-sourced Hg. Environ Sci Technol 47:2542–2547
44. Eiler JM, Bergquist B, Bourg I et al (2014) Frontiers of stable isotope geoscience. Chem Geol 372:119–143
45. Ridley WI, Stetson SJ (2006) A review of isotopic composition as an indicator of the natural and anthropogenic behavior of mercury. Appl Geochem 21:1889–1899
46. Sonke JE, Blum JD (2013) Advances in mercury stable isotope biogeochemistry. Chem Geol 336:1–4
47. Blum JD, Bergquist BA (2007) Reporting of variations in the natural isotopic composition of mercury. Anal Bioanal Chem 388:353–359
48. Lyons TW, Reinhard CT, Planavsky NJ (2014) The rise of oxygen in Earth/'s early ocean and atmosphere. Nature 506:307–315
49. Donovan PM, Blum JD, Yee D et al (2013) An isotopic record of mercury in San Francisco Bay sediment. Chem Geol 349:87–98
50. Yin R, Feng X, Meng B (2013) Stable mercury isotope variation in rice plants (*Oryza sativa* L.) from the Wanshan mercury mining district, SW China. Environ Sci Technol 47:2238–2245
51. Bartov G, Deonarine A, Johnson TM et al (2013) Environmental impacts of the Tennessee Valley Authority Kingston coal ash spill. 1. Source apportionment using mercury stable isotopes. Environ Sci Technol 47:2092–2099
52. Cooke CA, Hintelmann H, Ague JJ et al (2013) Use and legacy of mercury in the Andes. Environ Sci Technol 47:4181–4188
53. Day RD, Roseneau DG, Berail S et al (2012) Mercury stable isotopes in seabird eggs reflect a gradient from terrestrial geogenic to oceanic mercury reservoirs. Environ Sci Technol 46:5327–5335
54. Foucher D, Hintelmann H (2009) Tracing mercury contamination from the Idrija mining region (Slovenia) to the Gulf of Trieste using Hg isotope ratio measurements. Environ Sci Technol 43:33–39
55. Foucher D, Hintelmann H, Al TA et al (2013) Mercury isotope fractionation in waters and sediments of the Murray Brook mine watershed (New Brunswick, Canada): tracing mercury contamination and transformation. Chem Geol 336:87–95
56. Gehrke GE, Blum JD, Marvin-DiPasquale M (2011) Sources of mercury to San Francisco Bay surface sediment as revealed by mercury stable isotopes. Geochim Cosmochim Acta 75:691–705

57. Gehrke GE, Blum JD, Meyers PA (2009) The geochemical behavior and isotopic composition of Hg in a mid-Pleistocene western Mediterranean sapropel. Geochim Cosmochim Acta 73:1651–1665
58. Gray JE, Pribil MJ, Van Metre PC et al (2013) Identification of contamination in a lake sediment core using Hg and Pb isotopic compositions, Lake Ballinger, Washington, USA. Appl Geochem 29:1–12
59. Liu J, Feng X, Yin R et al (2011) Mercury distributions and mercury isotope signatures in sediments of Dongjiang, the Pearl River Delta, China. Chem Geol 287:81–89
60. Ma J, Hintelmann H, Kirk JL et al (2013) Mercury concentrations and mercury isotope composition in lake sediment cores from the vicinity of a metal smelting facility in Flin Flon, Manitoba. Chem Geol 336:96–102
61. Mil-Homens M, Blum J, Canário J et al (2013) Tracing anthropogenic Hg and Pb input using stable Hg and Pb isotope ratios in sediments of the central Portuguese Margin. Chem Geol 336:62–71
62. Perrot V, Epov VN, Pastukhov MV et al (2010) Tracing sources and bioaccumulation of mercury in fish of Lake Baikal–Angara River using Hg isotopic composition. Environ Sci Technol 44:8030–8037
63. Senn DB, Chesney EJ, Blum JD et al (2010) Stable isotope (N, C, Hg) study of methylmercury sources and trophic transfer in the northern Gulf of Mexico. Environ Sci Technol 44:1630–1637
64. Sherman LS, Blum JD (2013) Mercury stable isotopes in sediments and largemouth bass from Florida lakes, USA. Sci Total Environ 448:163–175
65. Sonke JE, Schäfer J, Chmeleff J et al (2010) Sedimentary mercury stable isotope records of atmospheric and riverine pollution from two major European heavy metal refineries. Chem Geol 279:90–100
66. Yin R, Feng X, Wang J et al (2013) Mercury isotope variations between bioavailable mercury fractions and total mercury in mercury contaminated soil in Wanshan Mercury Mine, SW China. Chem Geol 336:80–86
67. Yin R, Feng X, Wang J et al (2013) Mercury speciation and mercury isotope fractionation during ore roasting process and their implication to source identification of downstream sediment in the Wanshan mercury mining area, SW China. Chem Geol 336:72–79
68. Biswas A, Blum JD, Bergquist BA et al (2008) Natural mercury isotope variation in coal deposits and organic soils. Environ Sci Technol 42:8303–8309
69. Estrade N, Carignan J, Donard OFX (2011) Tracing and quantifying anthropogenic mercury sources in soils of northern France using isotopic signatures. Environ Sci Technol 45:1235–1242
70. Feng X, Yin R, Yu B et al (2013) Mercury isotope variations in surface soils in different contaminated areas in Guizhou Province, China. Chin Sci Bull 58:249–255
71. Shi W, Feng X, Zhang G et al (2011) High-precision measurement of mercury isotope ratios of atmospheric deposition over the past 150 years recorded in a peat core taken from Hongyuan, Sichuan Province, China. Chin Sci Bull 56:877–882
72. Blum JD, Anbar AD (2010) Mercury isotopes in the late Archean Mount McRae Shale. Geochim Cosmochim Acta 74:A98
73. Lefticariu L, Blum JD, Gleason JD (2011) Mercury isotopic evidence for multiple mercury sources in coal from the Illinois Basin. Environ Sci Technol 45:1724–1729
74. Sun R, Heimbürger L-E, Sonke JE et al (2013) Mercury stable isotope fractionation in six utility boilers of two large coal-fired power plants. Chem Geol 336:103–111
75. Das R, Bizimis M, Wilson AM (2013) Tracing mercury seawater vs. atmospheric inputs in a pristine SE USA salt marsh system: mercury isotope evidence. Chem Geol 336:50–61
76. Blum J, Johnson M, Gleason J et al (2012) Mercury concentration and isotopic composition of epiphytic tree lichens in the Athabasca oil sands region. Alberta Oil Sands: Energy, Industry and the Environment: Elsevier Press, Oxford, UK, pp 373–390
77. Estrade N, Carignan J, Donard OF (2010) Isotope tracing of atmospheric mercury sources in an urban area of northeastern France. Environ Sci Technol 44:6062–6067
78. Laffont L, Sonke JE, Maurice L et al (2009) Anomalous mercury isotopic compositions of fish and human hair in the Bolivian Amazon. Environ Sci Technol 43:8985–8990
79. Laffont L, Sonke JE, Maurice L et al (2011) Hg speciation and stable isotope signatures in human hair as a tracer for dietary and occupational exposure to mercury. Environ Sci Technol 45:9910–9916
80. Sherman LS, Blum JD, Franzblau A et al (2013) New insight into biomarkers of human mercury exposure using naturally occurring mercury stable isotopes. Environ Sci Technol 47:3403–3409
81. Tsui MTK, Blum JD, Kwon SY et al (2012) Sources and transfers of methylmercury in adjacent river and forest food webs. Environ Sci Technol 46:10957–10964
82. Gehrke GE, Blum JD, Slotton DG et al (2011) Mercury isotopes link mercury in San Francisco Bay forage fish to surface sediments. Environ Sci Technol 45:1264–1270
83. Kwon SY, Blum JD, Carvan MJ et al (2012) Absence of fractionation of mercury isotopes during trophic transfer of methylmercury to freshwater fish in captivity. Environ Sci Technol 46:7527–7534
84. Point D, Sonke J, Day R et al (2011) Methylmercury photodegradation influenced by sea-ice cover in Arctic marine ecosystems. Nat Geosci 4:188–194
85. Bigeleisen J (1996) Temperature dependence of the isotope chemistry of the heavy elements. Proc Natl Acad Sci USA 93:9393–9396
86. Angeli I (2004) A consistent set of nuclear rms charge radii: properties of the radius surface R (N, Z). At Data Nucl Data Tables 87:185–206
87. Young ED, Galy A, Nagahara H (2002) Kinetic and equilibrium mass-dependent isotope fractionation laws in nature and their geochemical and cosmochemical significance. Geochim Cosmochim Acta 66:1095–1104
88. Chen J, Hintelmann H, Dimock B (2010) Chromatographic preconcentration of Hg from dilute aqueous solutions for isotopic measurement by MC-ICP-MS. J Anal At Spectrom 25:1402–1409
89. Štrok M, Hintelmann H, Dimock B (2014) Development of preconcentration procedure for the determination of Hg isotope ratios in seawater samples. Anal Chim Acta 851:57–63
90. Wiederhold JG, Cramer CJ, Daniel K et al (2010) Equilibrium mercury isotope fractionation between dissolved Hg(II) species and thiol-bound Hg. Environ Sci Technol 44:4191–4197
91. Morel FM, Kraepiel AM, Amyot M (1998) The chemical cycle and bioaccumulation of mercury. Annu Rev Ecol Syst 29:543–566
92. O'Concubhair R, O'Sullivan D, Sodeau JR (2012) Dark oxidation of dissolved gaseous mercury in polar ice mimics. Environ Sci Technol 46:4829–4836
93. Selin NE (2009) Global biogeochemical cycling of mercury: a review. Annu Rev Environ Resour 34:43–63
94. Stohl A, Bonasoni P, Cristofanelli P et al (2003) Stratosphere–troposphere exchange: a review, and what we have learned from STACCATO. J Geophys Res Atmos (1984–2012) 108:D12
95. Sommerer TJ (1993) A Monte Carlo simulation of resonance radiation transport in the rare-gas-mercury positive column. J Appl Phys 74:1579–1589
96. Mughabghab S (2003) Thermal neutron capture cross sections resonance integrals and g-factors. International Atomic Energy Agency INDC(NDS)-440, Vienna
97. Bernards C, Urban W, Jentschel M et al (2011) γ γ angular-correlation analysis of 200 Hg after cold-neutron capture. Phys Rev C 84:047304
98. Inghram MG, Hess DC Jr, Hayden RJ (1947) Neutron cross sections for mercury isotopes. Phys Rev 71:561